

# Corrosion of rebar in carbon fiber reinforced polymer bonded reinforced concrete

Prasad V. Bahekar\* and Sangeeta S. Gadve<sup>a</sup>

Department of Applied Mechanics, Visvesvaraya National Institute of Technology, Nagpur-440010, India

(Received July 28, 2018, Revised April 10, 2019, Accepted June 6, 2019)

**Abstract.** Several reinforced concrete structures that get deteriorated by rebar corrosion are retrofitted using Carbon Fiber Reinforced Polymer (CFRP). When rebar comes in direct contact with CFRP, rebar may corrode, as iron is more active than carbon. Progression of corrosion of rebar in strengthened RC structures has been carried out when rebar comes in direct contact with CFRP. The experimentation is carried out in two phases. In phase I, corrosion of bare steel bar is monitored by making its contact with CFRP. In phase II, concrete specimens with surface bonded CFRP were casted and subjected to the realistic exposure conditions keeping direct contact between rebar and CFRP. Progression of corrosion has been monitored by various parameters: Half-cell potential, Tafel extrapolation and Linear Polarisation Resistance. On termination of exposure, to find residual bond stress between rebar and concrete, pull-out test was performed. Rebar in contact with CFRP has shown substantially higher corrosion. The level of corrosion will be more with more area of contact.

**Keywords:** reinforced concrete; rebar corrosion; Carbon Fiber Reinforced Polymer (CFRP); half-cell potential; corrosion rate (Icorr) Tafel Plots; linear polarisation resistance (LPR); bond stress; mass loss

## 1. Introduction

Reinforced Concrete (RC) is commonly used as construction material worldwide. Although proved reliable for a wide range of environmental conditions across the globe, there has been a number of structural failures before reaching its designed service life. One of the major causes of failure of RC is corrosion of reinforcing steel bars (rebar). Continuous availability of oxygen, moisture, chlorides and humid atmospheric conditions provide a favorable environment in accelerating corrosion.

Corrosion is the result of an electrochemical process having several chemical reactions with a flow of electrons. Anode, cathode and electrolyte are the essential parts of corrosion process. Since alkalinity of concrete surrounding reinforcing steel is much higher with a pH value of above 13, it provides a protective barrier against corrosion. (Broomfield 2007, ACI 222R-01 2001) Therefore, for initiation of corrosion this alkaline layer needs to be penetrated. The chloride ions help penetrates this alkaline layer for rebar to become an anode. (Neville and Brooks 2010) Thus, corrosion process is further accelerated if chlorides are also available in addition to oxygen and moisture. The corrosion products, thus produced, in various forms of hydrated iron oxides are much more voluminous as compared to the parent material and therefore exert pressure on the concrete surrounding the rebar, resulting in

cracking and eventual spalling of concrete. (Zhao *et al.* 2011, Uhlig and King 1972).

The steel and concrete bond gets affected; in certain cases, it may get completely lost (Zhou *et al.* 2017), also the bearing capacity of RC flexural members reduces. (Malerba 2017) Such corrosion damaged RC structures need repairs and rehabilitation to regain their original strength. Various methods for strengthening of corrosion affected RC structures are available; that may be employed depending upon several factors such as degree of deterioration, prevailing environmental conditions, ease of application of the method as well as expenditure involved. Using Fiber Reinforced Polymer (FRP) composites in strengthening of corrosion damaged RC members is one of the common methods nowadays. The composites, which are prepared using fibers surrounded by polymeric resin, are FRP. (ACI 440.2R 2008) Commonly used fiber types for strengthening purpose are Glass FRP (GFRP), Carbon FRP (CFRP) and Aramid FRP (AFRP). These FRPs in the form of sheets/wraps, laminates and bars are abundantly being used in the repair of RC structures.

FRP materials are lightweight, have high tensile strength to weight ratio and non-corrosive. (ACI 440.2R 2008) FRPs can resist acids, alkalis, salts for large temperature range. They also prohibit the entrance of humidity and corrosive chemicals. (Gadve *et al.* 2009) Flexural capacity of the beam can be enhanced by using externally bonded laminates or sheets as a replacement or add-on to the existing reinforcement. (Gadve *et al.* 2011, Attari *et al.* 2012, Sumathi and Arun 2017) Shear capacity of beams and columns may be improved by wrapping FRP sheets around the members. (Baggio *et al.* 2014, Kumutha *et al.* 2007, Pan *et al.* 2007) Among different FRP types, CFRP is found to be superior due to its inherent mechanical properties.

\*Corresponding author, Ph.D. Student  
E-mail: [prasad.bahekar@gmail.com](mailto:prasad.bahekar@gmail.com)

<sup>a</sup>Associate Professor  
E-mail: [sangeetagadve@gmail.com](mailto:sangeetagadve@gmail.com)

It is worth noting here that using FRP in strengthening of RC can resist corrosion effectively. The confinement provided by wrapping around FRP sheets, dodges expansion of RC corrosion, hence avoiding spalling. Wrapping of FRP sheet prevents the ingress of corrosion inducing elements, thereby providing passive protection to the rebar against corrosion. (Gadve *et al.* 2009) While enhancement in the structural performance of FRP strengthened components is well established, the process of corrosion in CFRP strengthened RC Structures forming galvanic cell is investigated by some investigators. Mehdi Yari (2017) has studied corrosion of mild steel coupled with CFRP in various environments. He reported that corrosion process of plain steel accelerates substantially in contact with CFRP in deicing solution and seawater. Torres-Acosta (2002) conducted experiments to investigate corrosion process of steel in contact with CFRP in chloride rich environment. Corrosion rate in steel rod attached to carbon epoxy was found to be 10 times that of bare steel rod. Mohammadreza (2001) studied corrosion of steel coupled with CFRP. He concluded that the corrosion of steel increases by multiple of 24 in de-icing salt solution and 57 in seawater when steel and carbon fibers coated with a thin film of epoxy are coupled together. In present study, progression of corrosion of rebar in CFRP strengthened RC structures is monitored, when rebar comes in contact with CFRP for various environments.

## 2. Experimental program

The experimental program was done in two phases. In Phase-I, a pilot study was carried out using bare steel bar and CFRP laminate. In Phase-II, the specimens simulating CFRP strengthened RC structures have been studied.

### 2.1 Phase-I

In the first phase, corrosion process in bare rebar exposed to chlorides has been investigated by considering three different exposure conditions, named as Case I, Case II, and Case III as follows:

Case I: Single bare rebar was kept in 3.5% NaCl to study the corrosion of steel bar subjected to chloride attack.

Case II: A bare rebar was connected to CFRP laminate using electrically conductive wire. They were kept together in 3.5% NaCl to study the corrosion process in steel bar when it comes in contact with CFRP laminate in chloride rich environment. An Ammeter was used for monitoring the flow of current.

Case III: A bare rebar and CFRP laminate were kept in direct contact with each other along the length, in 3.5% NaCl solution to find the effect of contact area on the process of corrosion. The two were kept together with the help of thread at two places.

Fig. 1 shows a schematic representation of the experimental setup with reference to the above mentioned three cases. Steel bar of grade Fe500 with nominal diameter 12 mm and length 180 mm was used. The 'STR Lam Strong' CFRP laminate provided by Speciality Reinforced Matrix Pvt. Ltd. Thane, of size 50 mm×180 mm was used.

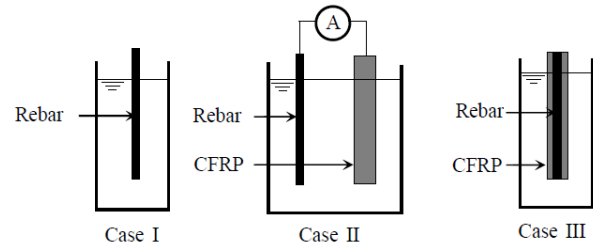


Fig. 1 Experimental Setup for Phase- I

Table 1 Mass loss at the end of exposure period

Specimen	Initial Weight gm	Final Weight gm	Mass Loss gm	Mass Loss %
Case I	156.180	155.530	0.650	0.416
Case II	155.779	154.290	1.489	0.956
Case III	153.168	150.950	2.218	1.448

The pilot study was continued for 51 days (1224 hours). The NaCl solution was changed intermittently to ensure ample supply of oxygen. Initial weight of all the samples was measured with the accuracy of  $\pm 1$  milligram.

#### 2.1.1 Monitoring

During entire exposure period, the following parameters were monitored in all three cases every day;

##### a) Half-cell potential

Rebar half-cell potential was monitored with reference to standard silver-silver chloride (Ag/AgCl) electrode (Song and Saraswathy 2007) in all the three cases every day. While observing the half-cell potential, steel bars were disconnected from CFRP laminate in Case II and Case III. The contact between CFRP and steel bars was disconnected by removing thread used for keeping them together.

##### b) Current flow between rebar and CFRP laminate

The flow of current between rebar and CFRP laminate in Case II was monitored every day. On the first day of exposure to saline environment, the current flowing from steel bar to CFRP laminate was found to be 0.5 mA. It went on increasing and became maximum at 0.88 mA on the 30th day of exposure. Thereafter, it remained constant for the remaining period of exposure.

##### c) Mass loss

At the end of the exposure duration, the bars were removed from the NaCl solution. The corrosion products accumulated on the bars were cleaned in accordance to ASTM G1-03. (ASTM G1 2003) The weight of the cleaned bars in all the three cases was measured to the accuracy of  $\pm 1$  milligram and the loss of mass calculated is presented in Table 1.

### 2.2 Phase-II

In Phase I of the experimentation, it has been established that when a steel bar comes in contact with CFRP, substantial current flows from steel to CFRP laminate. This clearly indicates that the flow of electrons

that ensues leads to the corrosion of rebar. In Phase II of the experimentation, an attempt was made to apply the same concept to realistic CFRP strengthened RC member. The procedures followed was:

- Preparation of test specimens
- Attaching CFRP to the specimens
- Exposing specimens to corrosive environment for a specified duration
- Corrosion monitoring of the specimens during the exposure period
- Destructive test on the specimens

### 2.2.1 Preparation of test specimens

Specimens used for the study were rectangular in cross-section. The cross-sectional of specimens was kept as 100 mm×100 mm and height as 200 mm with a concentrically fixed rebar having 12 mm diameter, as shown in Fig. 2. M<sub>45</sub> and Fe<sub>500</sub> grade of concrete and rebar respectively were used. M<sub>45</sub> grade of concrete was obtained by performing Concrete Mix Design as per IS10262:2009 (IS 10262 2009) for which OPC 53 cement was used. Natural river sand was used as fine aggregate and coarse aggregates has the size ranging from 20 mm to 4.75 mm. The ratio of cement: sand: coarse aggregate was 1:1.53:2.92 and the water-cement ratio was 0.45. The reinforcing bars were absolutely corrosion free. For maintaining white shining surface, the bars were kept in the oil immediately after manufacturing. Before embedding the steel bar in concrete during casting of the specimens, oil on surface was removed by cleaning it with acetone. A groove of 3 mm diameter was drilled in the cross-section of rebar at the top to plug copper stud in it for all necessary electrical connections. The rebar was coated with Teflon tape at the bottom 15 mm and top 171 mm to maintain exposed length of 130 mm in concrete. It also served as the bond breaker. The clear transverse cover of 44 mm was maintained on all sides as well as at the bottom. The special moulding system was fabricated to maintain uniform cover. After 24 hours, the specimens were removed from the moulds and the protruded rebar were coated with epoxy resin to avoid its exposure to air and moisture. The weights of rebar were noted before casting with the accuracy of ±1 milligram.

### 2.2.2 Attaching CFRP to the specimens

Carbon fiber reinforced polymers (CFRP) used for structural strengthening are available in various forms such as sheets/wraps, laminates and bars depending upon its application requirement. In the present study, CFRP laminates were used. After curing, specimens were dried and laminates were applied to one of the longitudinal surfaces in the direction parallel to reinforcing bar. Before applying CFRP laminate the surface was properly grinded to make it plain. Further, the surface was cleaned with acetone to make it dust free. Epoxy adhesive was used to bond the laminate with concrete surface in all cases except one where epoxy adhesive was modified to make it electrically conductive. CFRP laminate used in the experimentation was 200 mm long, 50 mm wide and 2 mm thick strip. The laminates were kept projecting above concrete top surface for about 20 mm. for enabling electrical connections.

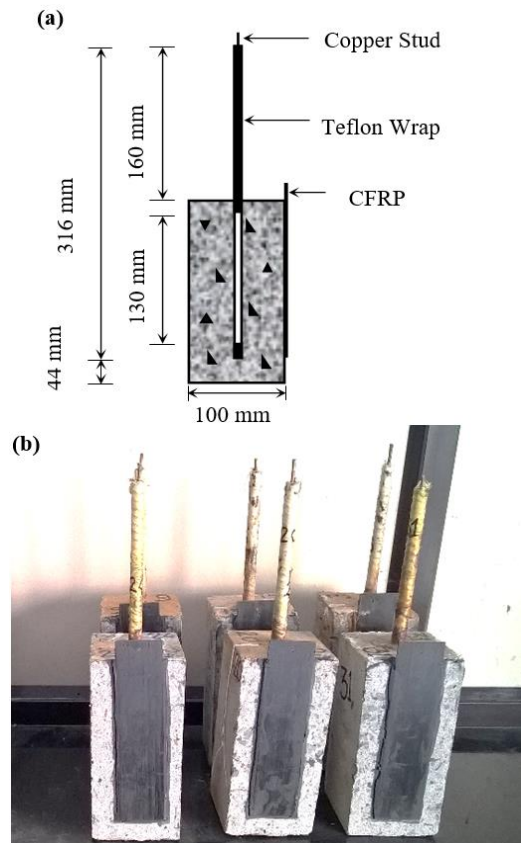


Fig. 2 Details of specimen in Phase II, (a) Schematic diagram (b) Specimens attached with laminates

### 2.2.3 Exposure to corrosive environment

To carry out an exhaustive investigation about the effect of corrosion on CFRP strengthened RC structural members the following cases were considered:

- Case I: Specimens without applying CFRP laminate were placed in tap water to simulate RC member subjected to a mild exposure condition. This was to study the possible corrosion of rebar in presence of residual chlorides of tap water while it was treated for domestic use.
- Case II: Specimens without applying CFRP laminates were placed in 3.5% NaCl to simulate RC member subjected to severe exposure condition such as offshore structures. This was to study the corrosion of rebar when it is exposed to saline environment.
- Case III: Specimens with surface bonded CFRP laminate were placed in tap water to simulate CFRP strengthened RC member subjected to a mild exposure condition to study the effect on corrosion of rebar same as in Case I.
- Case IV: Specimens with surface bonded CFRP laminate were placed in 3.5% NaCl to simulate RC member subjected to severe exposure condition to study the effect on corrosion of rebar same as in Case II.
- Case V: Specimens with surface bonded CFRP laminate were placed in 3.5% NaCl. In this case, adhesive was improved to make it electrically conductive so that the progression of corrosion in a conductive environment could be investigated.

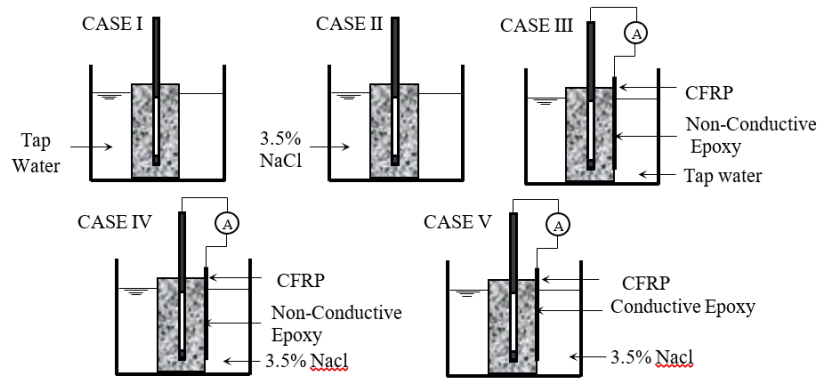


Fig. 3 Schematic diagram and actual Setup for exposure in Phase II

For each case, specimens were prepared in duplicate for each case.

Tap water used in Case I and Case III was from the same source. The ambient room temperature was maintained between 27°C to 30°C in all the cases throughout the exposure period. In Case III, Case IV and Case V, rebar and CFRP laminate were electrically connected as represented in Fig. 3, to simulate unintentional contact between two materials that might get established accidentally. The ammeter was also connected in between for monitoring the flow of current through the circuit. All the specimens were immersed in the prescribed exposure for the duration of 5400 hours (90 days). Tap water and saline solution was changed every 5 days to make sure the availability of oxygen for corrosive reactions.

#### 2.2.4 Monitoring

Corrosion monitoring was done by employing several destructive and non-destructive tests. Non-destructive tests included half-cell potential, Tafel plots (potentiodynamic scans) and linear polarization resistance, whereas destructive tests included pull-out test and mass loss test that was performed after the termination of exposure.

##### a) Half-cell potential

Half-cell potential of all the specimens was observed every day with Silver-Silver Chloride standard reference electrode (Ag/AgCl), for the entire exposure duration. The value of potential measured will depend on the grade of concrete, the availability of oxygen, thickness of corrosion. (Arup and Crane 1983, Wagner and Traud 1938, Dean 1976, Pradhan and Bhattacharjee 2009) Though it is a very rapid method of evaluating the corrosion, it does not give the actual rate of corrosion. To ensure the exact rate of corrosion half-cell potential should be used with other methods. (Mietz *et al.* 1998)

##### b) Tafel Plots

Tafel plots are used to find the corrosion rate  $I_{corr}$  at fixed interval. The corrosion rate is calculated to check the advancement in the corrosion process. The anodic and cathodic corrosion current at open circuit potential (OCP) can be related to the corrosion current  $i_{corr}$ . Rate of production of electric charges during the corrosion at anode is equal to the consumption of these charges at cathode so

to produce zero net current, to maintain the equilibrium. (Uhlig and King 1972, Wagner and Traud 1938, Dean 1976, Stern and Geary 1957, Al-Tayyib and Khan 1988, Stern and Weisert 1959)

In the present study, Tafel plots were obtained from all specimens on a Potentiostat (VersaSTAT-3, AMETEK), every fortnight throughout the exposure period. Ag/AgCl was used as a reference, stainless steel wire mesh as counter electrode and the rebar was acting as a working electrode. The scan rate of 0.1666 mV/s was maintained, with step height of 0.5 mV and step time of 3 seconds. The applied potential was  $\pm 250$  mV at OCP. Instantaneous corrosion rate  $I_{corr}$ , is obtained from the Tafel plots.

##### c) Linear Polarization Resistance (LPR)

Polarization Resistance can be called as the resistance of the specimen to external potential. For evaluating the corrosion current density, LPR is a widely used technique. (Gonzalez *et al.* 1985, El-Gelany 2001, Dehwah *et al.* 2002, Saricimen *et al.* 2002, Erdođdu *et al.* 2001, Andi3n 2001, Almutlaq 2014). Scan rate was maintained at 0.1666 mV/s as in case of Tafel, however, the step height was kept at 1 mV with 0.6 seconds step time,  $\pm 20$  mV at OCP was the potential applied. The current obtained was plotted against corresponding potential, which turns out to be a straight line from which  $I_{corr}$  is calculated. The experimental setup used to obtain Tafel plots and LPR is shown in Fig. 4.

The CFRP and rebar were disconnected during the experimental procedures of the LPR and Tafel techniques. So, the polarization resistance data are from the rebar only. In the present study, before measurement of Tafel plots, CFRP and rebar were disconnected and allowed to stabilize for more than four hours. On completion of Tafel, once again the specimens were stabilized for four hours before measuring LPR.

##### d) Destructive Tests

In addition to the Non-destructive corrosion measuring parameters such as half-cell potential, Tafel plots and LPR measurements as mentioned above, destructive methods such as pull-out test and mass loss determination were also employed.

After 90 days of exposure, pull-out test was carried out using Auto UTM (HEICO) (Fig. 5) by applying the load rate of 0.2 kN/second. The pull-out test was carried out in

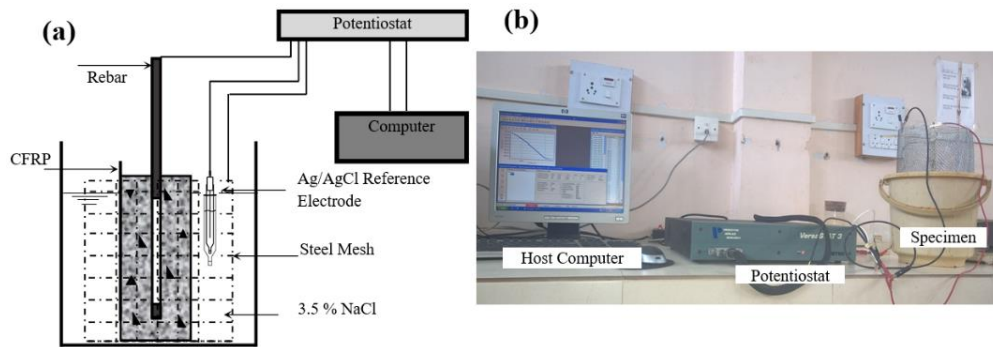


Fig. 4 Setup for Tafel plots and LPR (a) Schematic, (b) Experimental

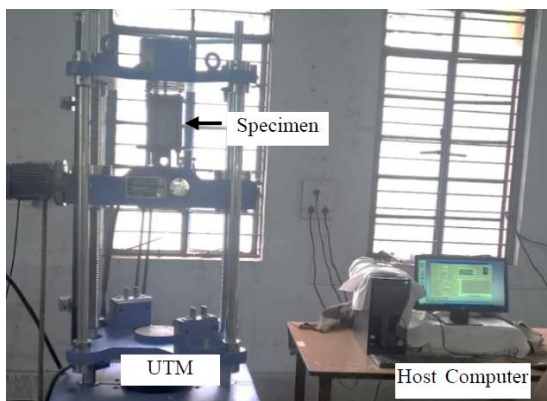


Fig. 5 Experimental setup for pull out test

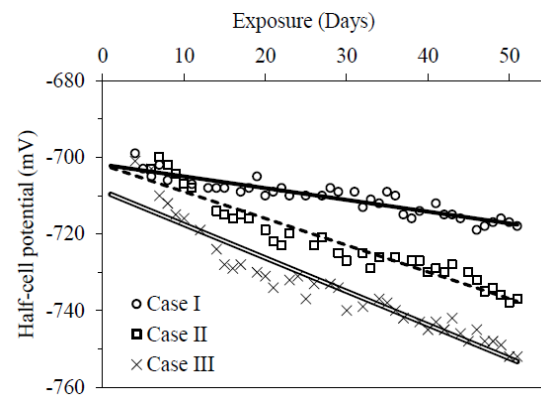


Fig. 6 Half-Cell values with respect to Ag-AgCl electrode

accordance with IS 2770 (Part I) 1967 (IS: 2770 Part I - 1967).

RC specimen was kept between two rigid steel plates connected by high strength bolts. Lower plate with projection was fixed into the lower jaw and the rebar was fixed in the upper jaw of UTM. Maximum pull out load and corresponding slip were noted. After the reinforcing bars are completely pulled out of the concrete matrix in pull out test, the rebar is thoroughly cleaned off corrosion products as per ASTM G-1 90 17 and weighed to the accuracy of  $\pm 0.1$  milligram). Mass loss is calculated by subtracting the weight of corroded rebar from the corresponding initial weight of the same rebar.

### 3. Results and discussion

#### 3.1 Phase I

The half-cell potential values were recorded every day for all three cases. As the scatter was observed in half cell potentials, a linear fit was obtained discarding the extreme half-cell potential values. Fig. 6 shows a variation of half-cell potential with respect to exposure duration. In all the three cases, the potential went down clearly indicating the progression of corrosion, albeit with different rates of downward movement. Case I, representing natural corrosion in chloride rich environment, showed the lowest rate as compared to the other two cases. In both Case II and case III, where a steel bar was connected to CFRP laminate, higher negative half-cell potential values were observed as

compared to Case I. This finding indicates that the corrosion process accelerates when a steel bar comes in contact with CFRP, due to easy and uninterrupted ionic movement. An additional finding was that Case III showed higher negative values as compared to Case II, indicating that corrosion is aggravated with an increased area of contact between steel bar and Carbon laminate. Availability of more surface area appears to have caused enhanced oxidation of rebar. Furthermore, in Case II the loss of current flowing is likely to be the effect of resistance in a circuit that slowed down the corrosion reaction. These results are alarming for repairs and retrofitting industry employing CFRP composites. In view of this, it is necessary to be extremely careful while applying CFRP systems to the corrosion damaged RC structures. The repair/rehabilitation or strengthening of such structures may cause further deterioration due to corrosion if a direct contact is established between steel reinforcement and CFRP composites, though accidentally.

In Case II, where steel bar and CFRP laminate are connected through electrically conductive wire, an ammeter was also connected in series for measuring current flowing between the two materials. The ammeter showed the direction of flow of current from steel bar to CFRP laminate. The indication of the flow of electrons from steel to carbon established that the corrosion of steel bar was in progress. At the beginning of the experiment, on the very first day of exposure to the corrosive environment, the current flowing from steel bar to CFRP laminate observed on ammeter was  $0.5 \text{ mA}$  (Current Density= $7.46 \mu\text{A}/\text{cm}^2$ ). During the next 40 days of exposure, a continuous increase

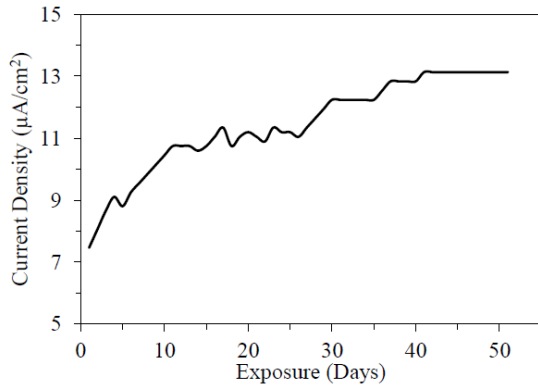


Fig. 7 Current density variation in Case II (Phase-I) throughout exposure

in the flow of current was recorded reaching a maximum at 0.88 mA (Current Density=13.13  $\mu\text{A}/\text{cm}^2$ ). On further exposure, however, the current flowing between the two materials was found to be almost constant till the end of experimentation. These findings are shown in Fig. 7.

At the end of the exposure period, the corroded bars were cleaned of corrosion products and weighed to the accuracy of  $\pm 1$  milligram. Table 1 presents the percentage mass loss in all the three cases. From the results of mass loss, a similar pattern in the extent of corrosion with reference to half-cell potentials is observed in all three cases. Mass loss is highest in Case III and lowest in Case I. In Case II, loss of mass in steel by the corrosion resulting from contact of steel bar with CFRP is 130% more as compared to loss of mass in steel bar due to natural corrosion in chloride rich environment. It may be further deduced that the area of contact between the anode and cathode also influences the extent of corrosion as mass loss in Case III is 51% higher as compared to Case II.

### 3.2 Phase II

The scatter of half-cell potential readings plotted against exposure duration shows down trend that clearly indicates progress of rebar corrosion in all specimens (Fig. 8). A linear fit is obtained to further compare the results. The slope of the linear fit in Case I and Case II is lower as compared to the slope of the linear fit in Case III, Case IV and Case V. It may be recalled here that if rebar and strengthening CFRP material comes in contact, corrosion of rebar accelerates. Further, to study the effect of exposure condition on corrosion of rebar, Case I and Case II results can be compared. It is clearly seen that RC specimens subjected to chloride rich severe exposure condition corrode more than the one subjected to mild exposure conditions. A similar trend is observed in Case III, Case IV and Case V. Case IV and Case V are identical, except in relation to the use of non-conductive and conductive epoxy adhesive for bonding CFRP laminates. When compared, Case V shows higher negative potentials than Case IV, indicating that the conductive epoxy helped electrons move faster than in non-conductive epoxy, thereby accelerating the corrosion process in Case V. The average current density value obtained at the end of exposure in CASE III, CASE IV and

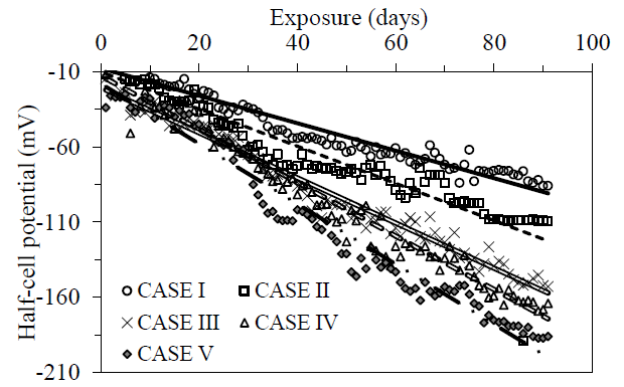


Fig. 8 Half-cell values of rebar with respect to Ag-AgCl electrode

Table 2 (a) Corrosion current by LPR

Exposure (hr)	$I_{corr}$ ( $\mu\text{A}/\text{cm}^2$ ) by LPR				
	CASE I	CASE II	CASE III	CASE IV	CASE V
360	0.0228	0.0257	0.0232	0.022	0.0265
720	0.0235	0.0262	0.0238	0.0256	0.0308
1080	0.0242	0.0253	0.0268	0.0335	0.0368
1440	0.0281	0.0283	0.033	0.0374	0.0346
1800	0.0288	0.0301	0.0335	0.0387	0.0466
2160	0.0306	0.0326	0.0376	0.0404	0.0491

Table 2 (b) Corrosion current by Tafel plot

Exposure (hr)	$I_{corr}$ ( $\mu\text{A}/\text{cm}^2$ ) by Tafel				
	CASE I	CASE II	CASE III	CASE IV	CASE V
360	0.0238	0.0286	0.0219	0.0278	0.0253
720	0.0248	0.0258	0.0312	0.0288	0.0355
1080	0.0292	0.0294	0.0343	0.0456	0.0543
1440	0.0355	0.0369	0.0479	0.0557	0.052
1800	0.0357	0.0389	0.0499	0.0568	0.0647
2160	0.0375	0.0421	0.0539	0.0619	0.068

CASE V were 0.0047  $\mu\text{A}/\text{cm}^2$ , 0.0076  $\mu\text{A}/\text{cm}^2$ , 0.01  $\mu\text{A}/\text{cm}^2$  respectively.

Tafel Plots as well as LPR measurement are performed to obtain corrosion current,  $I_{corr}$  ( $\mu\text{A}/\text{cm}^2$ ). Average  $I_{corr}$  obtained from Tafel Plots and LPR measurements at various exposure duration are presented in Table 2(a) and Table 2(b), respectively. Variation of  $I_{corr}$  with the period of exposure as obtained from Tafel plots and LPR measurement are shown in Fig. 9(a) and Fig. 9(b), respectively.

From Fig. 9(a) and Fig. 9(b), it can be clearly seen that  $I_{corr}$  is directly proportional to the exposure period in all the cases.  $I_{corr}$  obtained by both the methods show similar trends. The rate of increase of  $I_{corr}$  is highest in Case V and lowest in Case I, as expected. Case II shows a higher corrosion rate as compared to Case I, whereas Case IV shows a higher corrosion rate as compared to Case III, thereby proving that the presence of chlorides expedites the corrosion process. It is once again observed that use of conductive epoxy adhesive accelerates progression of corrosion.

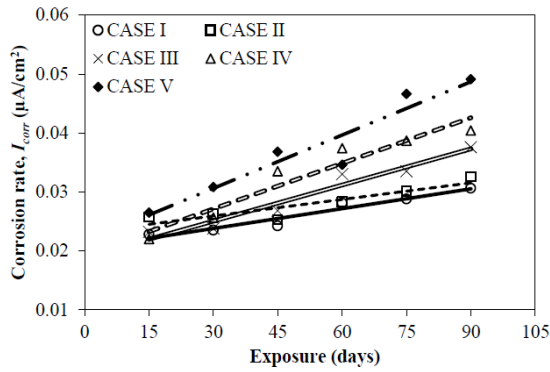
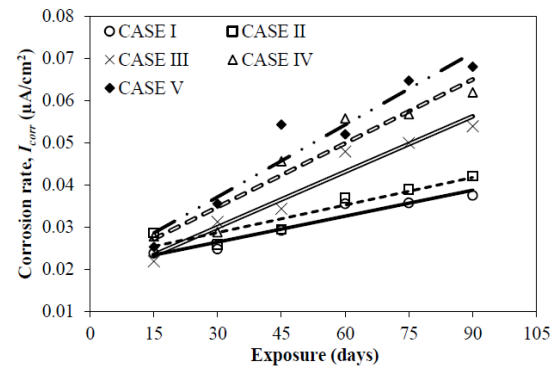
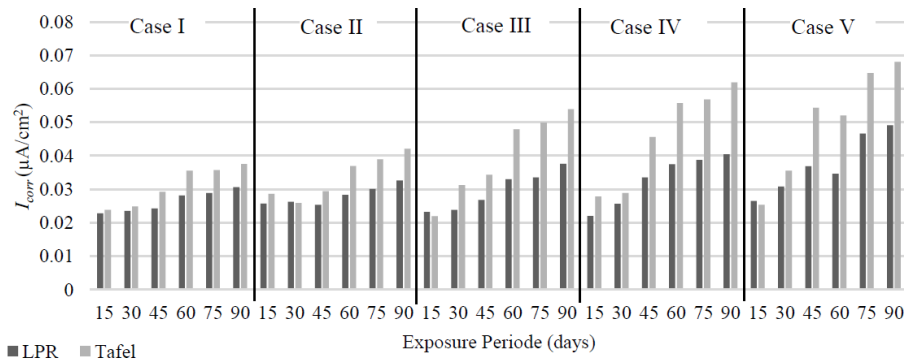
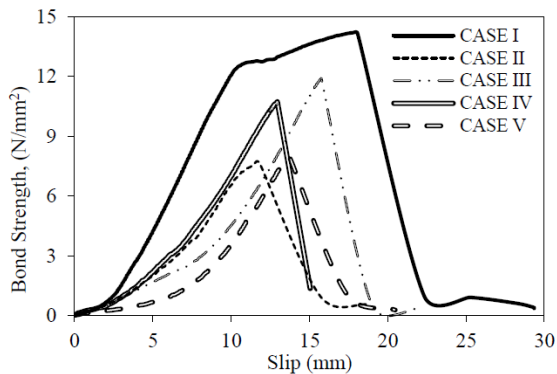
Fig. 9(a) Plot of  $I_{corr}$  versus exposure time by LPRFig. 9(b) Plot of  $I_{corr}$  versus exposure time by TafelFig. 10 Comparison of  $I_{corr}$  for various cases throughout exposure period

Fig. 11 Variation of pull-out strength and slip

Although the trend in the increase of  $I_{corr}$  with the duration of exposure period is found to be similar in both methods, that is Tafel and LPR, it can be observed that the  $I_{corr}$  obtained from Tafel plot measurement is higher than the  $I_{corr}$  obtained from the LPR for the same specimen (Fig. 10). It is also observed that during the initial exposure period, both methods give almost similar  $I_{corr}$ . However, with an extension in exposure period, the difference in the  $I_{corr}$  obtained from both methods keeps on increasing. For the initial period of exposure up to 30 days, the average percentage difference in  $I_{corr}$  obtained from both the methods is about 10%, which increases to about 37% towards the end of the exposure period.

Researchers have not used both the methods simultaneously on the same specimens. However, it would be interesting to explore the variations in the  $I_{corr}$  obtained from two different methods. After evaluating corrosion by

Table 3 Bond strength with respective slip and actual mass loss at the end of exposure period

CASE	I	II	III	IV	V
Mass loss, (gm)	0.0026	0.003	0.0032	0.0039	0.0043
Mass loss, (%)	0.0024	0.0027	0.0029	0.0035	0.0039
Bond strength, (N/mm <sup>2</sup> )	14.167	12.37	11.90	10.71	7.85
Slip, (mm)	18.07	11.82	15.76	12.95	13.78

non-destructive parameters, pull out test was performed, and Bond strength versus Slip curves are obtained for all the specimens as shown in Fig. 11.

Average bond Strength values and slip values presented in Table 3, shows that the highest bond strength is obtained for Case I and the Lowest is obtained for Case V. This is as expected. Variation in the bond strength-slip values is decreasing from Case I to Case V.

The average mass loss as presented in Table 3 is continuously decreasing from Case I to Case V. This is in complete agreement with all the corrosion measuring parameters that have been discussed earlier. Mass loss due to corrosion is found to be 15% higher in chloride rich severe exposure as in Case II compared to mild exposure as in Case I. In the cases where rebar and CFRP are in contact with each other, mass loss due to corrosion is found to be 21% higher in chloride rich severe exposure as compared to mild exposure in Case III and Case IV. Higher mass loss is observed in later cases due to twofold corrosion occurring in Case IV and Case V, that is corrosion due to chloride attack and corrosion due to the direct connection between rebar and CFRP.

#### 4. Conclusions

Based on the results, the following conclusions are drawn:

- Corrosion of the rebar is almost 15% higher when it is subjected to chloride rich severe exposure as compared to mild exposure conditions.
- When rebar comes in direct contact with the material having higher potential value than steel (Fe), such as Graphite (Carbon), in the presence of oxygen and moisture, electrons flow from rebar to CFRP, thereby causing corrosion of rebar.
- In view of the above conclusion, there lies a risk of corrosion damage in CFRP strengthened RC structures, if the CFRP strengthening material comes in contact with rebar, albeit unintentionally or accidentally.
- Rebar corrosion is further aggravated while it is in contact with CFRP in chloride rich environment.
- The contact area between CFRP and rebar is directly proportional to the level of corrosion in rebar.
- Corrosion of rebar is higher in case of CFRP strengthened RC structures, in which conductive epoxy adhesive is used for surface bonding as compared to using nonconductive epoxy adhesive.
- Corrosion rate ( $I_{corr}$ ) determined from Tafel plots are higher than  $I_{corr}$  obtained from LPR measurements and the difference increases with an increase in exposure period.

#### Acknowledgments

The authors would like to thank Dr. A. P. Patil, Professor, VNIT, Nagpur for making Corrosion laboratory available to perform the Potentiostat scans. We would also like to express sincere appreciation towards MHRD, Government of India for making funds available through TEQIP-II. Authors would like to express sincere appreciation to Krishna Conchem pvt. ltd. and Dr. Mangesh Joshi, Speciality Reinforced Matrix Pvt. Ltd for providing epoxy adhesives for the study.

#### References

- ACI Committee 222 (2002), Protection of metal in concrete against corrosion, ACI 222R-01, American Concrete Institute, Farmington Hills, 8.
- ACI Committee 440 (2008), Guide for the design and construction of externally bonded FRP systems for strengthening concrete structures, (ACI 440.2R), American Concrete Institute, Farmington Hills, 12-15.
- Al-Tayyib, A.H.J. and Khan, S. (1988), "Corrosion rate measurements of reinforcing steel in concrete by electrochemical techniques", *Mater. J. Am. Concrete Inst.*, **85**(3), 172-177.
- Almutlaq, F.M. (2014), "The influence of EAF dust on resistivity of concrete and corrosion of steel bars embedded in concrete", *Adv. Concrete Constr.*, **2**(3), 163-176.
- Andión, L.G., Garcés, P., Cases, F., Andreu, C.G. and Vazquez, J.L. (2001), "Metallic corrosion of steels embedded in calcium aluminate cement mortars", *Cement Concrete Res.*, **31**(9), 1263-1269.
- Arup, H. and Crane, A.P. (1983), *Corrosion of Reinforcement in Concrete Construction*, The Society of Chemical Industry, Chichester, London, UK.
- ASTM G1-90 (1999), Standard Practice for Preparing, Cleaning, and Evaluating Corrosion Test Specimens, American Society for Testing and Materials, West Conshohocken, 20.
- Attari, N., Amziane, S. and Chemrouk, M. (2012), "Flexural strengthening of concrete beams using CFRP, GFRP and hybrid FRP sheets", *Constr. Build. Mater.*, **37**, 746-757.
- Baggio, D., Soudki, K. and Noel, M. (2014), "Strengthening of shear critical RC beams with various FRP systems", *Constr. Build. Mater.*, **66**, 634-644.
- Broomfield, J.P. (2007), *Corrosion of Steel in Concrete: Understanding, Investigation and Repair*, Taylor & Francis, 2<sup>nd</sup> Edition, Great Britain.
- Dean, Jr. S.W. (1977), "Electrochemical methods of corrosion testing", Paper, Electrochemical Techniques for Corrosion, National Association of Corrosion Engineers, Houston, 52-60.
- Dehwah, H.A.F., Maslehuddin, M. and Austin, S.A. (2002), "Long-term effect of sulfate ions and associated cation type on chloride-induced reinforcement corrosion in Portland cement concretes", *Cement Concrete Compos.*, **24**(1), 17-25.
- El-Gelany, M.A. (2001), "Short-term corrosion rate measurement of OPC and HPC reinforced concrete specimens by electrochemical techniques", *Mater. Struct.*, **34**(7), 426-432.
- Erdoğan, Ş., Bremner, T.W. and Kondratova, I.L. (2001), "Accelerated testing of plain and epoxy-coated reinforcement in simulated seawater and chloride solutions", *Cement Concrete Res.*, **31**(6), 861-867.
- Gadve, S., Mukherjee, A. and Malhotra, S.N. (2009), "Corrosion of steel reinforcements embedded in FRP wrapped concrete", *Constr. Build. Mater.*, **23**(1), 153-161.
- Gadve, S., Mukherjee, A. and Malhotra, S.N. (2011), "Active protection of fiber-reinforced polymer-wrapped reinforced concrete structures against corrosion", *Corros.*, **67**(2), 025002-1.
- Gonzalez, J.A., Molina, A., Escuder, M.L. and Andrade, C. (1985), "Errors in the electrochemical evaluation of very small corrosion rates-I. polarization resistance method applied to corrosion of steel in concrete", *Corros. Sci.*, **25**(10), 917-930.
- IS 10262 (2009), Concrete Mix Proportioning-Guidelines, IS 10262: 2009, Bureau of Indian Standards, New Delhi, India.
- IS2770 (Part I) (1967), Methods of Testing Bond in Reinforced Concrete Part I Pull-Out Test, (IS: 2770 (Part I) - 1967), Bureau of Indian Standards, New Delhi, India.
- Kumutha, R., Vaidyanathan, R. and Palanichamy, M.S. (2007), "Behaviour of reinforced concrete rectangular columns strengthened using GFRP", *Cement Concrete Compos.*, **29**(8), 609-615.
- Malerba, P.G., Sgambi, L., Ielmini, D. and Gotti, G. (2017), "Influence of corrosive phenomena on bearing capacity of RC and PC beams", *Adv. Concrete Constr.*, **5**(2), 117-143.
- Mietz, J., Elsener, B. and Polder, R. (1998), *Corrosion of Reinforcement in Concrete. Monitoring, Prevention and Rehabilitation*, The Institute of Materials Minerals and Mining.
- Neville, A.M. and Brooks, J.J. (2010), *Concrete Technology*, Pearson Education Limited, England, 2<sup>nd</sup> Edition, 270-271.
- Pan, J.L., Xu, T. and Hu, Z.J. (2007), "Experimental investigation of load carrying capacity of the slender reinforced concrete columns wrapped with FRP", *Constr. Build. Mater.*, **21**(11), 1991-1996.
- Pradhan, B. and Bhattacharjee, B. (2009), "Performance evaluation of rebar in chloride contaminated concrete by corrosion rate", *Constr. Build. Mater.*, **23**(6), 2346-2356.
- Saricimen, H., Mohammad, M., Quddus, A., Shameem, M. and Barry, M.S. (2002), "Effectiveness of concrete inhibitors in

- retarding rebar corrosion”, *Cement Concrete Compos.*, **24**(1), 89-100.
- Song, H.W. and Saraswathy, V. (2007), “Corrosion monitoring of reinforced concrete structures-a”, *Int. J. Electrochem. Sci.*, **2**, 1-28.
- Stern, M. and Geary, A.L. (1957), “Electrochemical polarization I. A theoretical analysis of the shape of polarization curves”, *J. Electrochem. Soc.*, **104**(1), 56-63.
- Stern, M. and Weisert, E.D. (1959), “Experimental observations on the relation between polarization resistance and corrosion rate”, *Proc. American Society of Testing Materials*, **59**, 1280.
- Sumathi, A. and Arun, V.S. (2017), “Study on behavior of RCC beams with externally bonded FRP members in flexure”, *Adv. Concrete Constr.*, **5**(6), 625-638.
- Tavakkolizadeh, M. and Saadatmanesh, H. (2001), “Galvanic corrosion of carbon and steel in aggressive environments”, *J. Compos. Constr.*, **5**(3), 200-210.
- Torres-Acosta, A.A. (2002), “Galvanic corrosion of steel in contact with carbon-polymer composites. II: Experiments in concrete”, *J. Compos. Constr.*, **6**(2), 116-122.
- Uhlig, H.H. and King, C.V. (1972), “Corrosion and corrosion control”, *J. Electrochem. Soc.*, ECS, **119**(12), 327C-327C.
- Wagner, C. and Traud, W. (1938), “On the interpretation of corrosion processes through the superposition of electrochemical partial processes and on the potential of mixed electrodes”, *Zeitschrift für Electrochemie, ZEELA*, **44**, 391.
- Yari, M. (2017), “Galvanic corrosion of metals connected to carbon fiber reinforced polymers”, April 18, 2017.
- Zhao, X., Gong, P., Qiao, G., Lu, J., Lv, X. and Ou, J. (2011), “Brillouin corrosion expansion sensors for steel reinforced concrete structures using a fiber optic coil winding method”, *Sensor. Basel, Switzerland*, **11**, 10798-10819.
- Zhou, H., Liang, X., Wang, Z., Zhang, X. and Xing, F. (2017), “Bond deterioration of corroded steel in two different concrete mixes”, *Struct. Eng. Mech.*, **63**(6), 725-734.